Journal of ELECTRONIC MATERIALS, Vol. 48, No. 12, 2019
https://doi.org/10.1007/s11664-019-07625-5
© 2019 The Minerals, Metals & Materials Society

Magnetic, Electronic, Mechanic, Anisotropic Elastic and Vibrational Properties of Antiferromagnetic Ru_2TGa (T = Cr, Mn, and Co) Heusler Alloys

A. CANDAN [1,2]

1.—Department of Machinery and Metal Technology, Ahi Evran University, 40100 Kırşehir, Turkey. 2.—e-mail: acandan@ahievran.edu.tr

A theoretical study of magnetic, electronic, mechanic, anisotropic elastic, and vibrational properties of Ru_2TGa (T = Cr, Mn, and Co) Heusler alloys has been extensively investigated by the first-principles method using the generalized gradient approximation. Structural parameters such as lattice constant (a_0), bulk modulus (B) and first pressure derivative of bulk modulus (B') were obtained by using the Murnaghan equation. The calculated formation enthalpies (ΔH_f) showed that these alloys are thermodynamically stable. The total spin magnetic moments per unit cell of Ru_2TGa (T = Cr, Mn, and Co) alloys were found to be 1.16 μ_B, 2.16 μ_B and 0.29 μ_B, respectively. In addition to electronic band structures along the high symmetry directions, corresponding total and partial density of states were also plotted. It was found that the spin-up states have a metallic character for all alloys, but the spin-down states of the other alloys except for Ru_2CoGa have a pseudo-gap at the Fermi level. The bulk modulus (B), shear modulus (G), ratio of B/G, Young's modulus (E), Poisson's ratios (ν), Vickers hardness (H_V), sound velocities (v_l, v_t, and v_m), Debye temperatures (Θ_D) and melting temperatures (T_{melt}) were obtained from elastic constants (C_{ij}) in accordance with the Voigt–Reuss–Hill approximation. The calculated elastic constants showed that these alloys are mechanically stable and they have anisotropic character. The elastic anisotropy of the considered alloys was analyzed and pictured in great detail with 2D and 3D figures of directional dependence of Young's modulus, linear compressibility, shear modulus, and Poisson's ratio.These alloys are dynamically stable because there are no negative modes in their phonon dispersion curves.

Key words: Antiferromagnetics, Heusler alloys, electronic properties, mechanical properties, phonon dispersion

INTRODUCTION

Heusler type alloys were discovered by Friedrich Heusler, a German mining engineer and chemist, at the beginning of the 1900s.[1] These alloys were obtained by adding a third group element to CuMn alloy; researchers observed that by performing such additions, the ferromagnetic properties of the alloying elements could be changed.[2,3] The resulting alloys are classified into two different groups as half and full Heusler alloys. These alloys are specified by the general formula ABC and A_2BC, respectively. Full-Heusler type alloys are ternary intermetallic compounds with stoichiometric composition A_2BC and $L2_1$ type cubic crystal structure. The A and B elements are from the transition metal group of the periodic table, whereas the C element belongs to the group III-V of the periodic table. Recently, Heusler

(Received April 19, 2019; accepted September 5, 2019; published online September 17, 2019)

type alloys are attracting researchers' attention due to their interesting magnetic properties. Half-metallic ferromagnets, which are the focus of scientific studies because of their potential applications in the field of spintronics,[4] were discovered in 1983 by De Groot et al.[5] Due to their half-metallic behavior, Heusler type alloys comprise an ideal material group for use in many electronic devices.[6] The main topics studied on Heusler type alloys include magnetic susceptibility and permeability, shape changes caused by magnetic field application, Curie temperature, hysteresis curves, magneto-optic Kerr effect, Hall phenomenon and ferromagnetic resonance.[7–10]

Up to this day, Heusler type alloys have been the subject of many studies.[11–22] However, an extensive study about the physical properties of the Ru_2TGa (T = Cr, Mn, and Co) Heusler alloys has not yet been made. The mechanical and vibrational properties of these materials have hardly been studied compared to other Heusler alloys. Ru_2TGa (T = Cr, Mn, and Co) Heusler alloys have been the subject of few theoretical and experimental studies.[23–30] Experimentally, the standard enthalpies of formation, lattice parameters, and phase transitions of Ru_2YZ (Y = Mn, Co, Fe, Hf, Rh, Ti, V, Zr; Z = Ga, Al, In, Si, Ge, Sn) Heusler compounds were analyzed by Yin and Nash.[23] They measured standard formation enthalpy for the Ru_2MnGa alloy by employing direct reaction calorimetry at high temperatures. Moreover, they determined the lattice parameters of Ru_2MnGa with x-ray diffraction analysis. In another experimental study, Hori et al. realized neutron diffraction data of the Ru_2MnGa alloy using Rietveld method.[24] They concluded that Mn mainly occupied one site (92.6%), showing it either had $L2_1$ or $D0_3$ structure. They also confirmed the stability of Ru_2MnGa in $L2_1$-type structure and its anti-ferromagnetic behavior. On the theoretical side, M. Gilleßen studied the lattice constants and magnetic moments of Ru_2TGa (T = Cr, Mn, and Co) Heusler alloys using density functional theory (DFT).[26] The lattice constants of these alloys have been reported as 5.994 Å, 5.996 Å, and 5.940 Å, respectively. Faleev et al. have investigated the chemical order and magnetic properties of numerous cubic full Heusler alloys, including the Ru_2MnGa alloy, which is one of the most promising candidates for half-metallicity.[27] They developed an orbital coupling model for cubic full Heusler compounds in their study. In another study recently conducted by the same authors, the lattice constant and magnetic moment of the Ru_2MnGa alloy in the tetragonal phase were calculated using DFT.[28] Jan Balluff in his Ph.D. thesis obtained a detailed dataset with DFT of the 70 antiferromagnetic Heusler compounds, including the Ru_2CrGa alloy.[29] He found the lattice constant and magnetic moment of the antiferromagnetic Ru_2CrGa alloy as 5.993 Å and 1.5 μ_B, respectively.

To the best of our knowledge, a comprehensive study of the physical properties of the Ru_2CrGa, Ru_2MnGa, and Ru_2CoGa Heusler alloys has not been performed to date. In particular, there is no experimental study in the literature about the Ru_2CrGa and Ru_2CoGa alloys. However, I found that these alloys have negative formation enthalpy, which indicates experimental synthesizability; therefore, this study can lead to future experimental studies. The aim of this study is to investigate the magnetic, electronic, mechanic, anisotropic elastic and vibrational properties of Ru_2TGa (T = Cr, Mn, and Co) Heusler alloys used as spintronic materials in potential applications.

Calculation methods for Ru_2TGa (T = Cr, Mn, and Co) alloys are presented in the second section. The third section presents the obtained magnetic, mechanic, anisotropic elastic and vibrational properties, and also electronic band structure properties of Ru_2TGa (T = Cr, Mn, and Co) alloys.

METHOD OF CALCULATION

The structural, electronic, magnetic, and elastic properties of antiferromagnetic Ru_2TGa (T = Cr, Mn, and Co) Heusler alloys were calculated by applying the self-consistent ultrasoft pseudopotential method.[31] The exchange–correlation potential was described as a generalized gradient approach[32,33] within the form recommended by Perdew-Burke-Ernzerhof.[34] All calculations were carried out with Quantum-Espresso[35] software based upon density functional theory (DFT).[36,37] First, the lattice constants in the frame of the structural parameters were obtained, then the bulk modulus and first pressure derivative of the bulk modulus were calculated by fitting the total energy as a function of the volume to the Murnaghan equation of states.[38] To obtain the equilibrium lattice constant of Ru_2TGa (T = Cr, Mn, and Co) alloys, the total energies corresponding to different lattice constant values were calculated by taking the 40 Ryd cut-off energy. For Brillouin zone integrations, a mesh of $12 \times 12 \times 12$ Monkhorst–Pack[39] k-points was used. Integration up to the Fermi surface was performed using the smearing technique[40] together with smearing parameter $\sigma = 0.01$ Ry. The elastic constants were calculated from the total energy change by applying small strains to the equilibrium lattice configuration.[41,42] In order to find the self-consistent solutions of the Kohn–Sham equations, the lattice dynamical properties were calculated according to the density functional perturbation theory.[43] With a view to obtaining full phonon dispersions along the high symmetry directions, eight dynamic matrices were computed on a $4 \times 4 \times 4$ q-point mesh. These dynamic matrices in arbitrary wave vectors were explained using inverse Fourier transform for this mesh.

RESULTS AND DISCUSSION

Crystal Structure and Formation Enthalpy

The unit cell of the full-Heusler-type alloys in the form of A_2BC with Cu_2MnAl type cubic structure and space group Fm-3m (No. 225) contains four fcc sublattices at coordinates (0, 0, 0) and (0.5, 0.5, 0.5) for atom A, (0.25, 0.25, 0.25) for atom B and (0.75, 0.75, 0.75) for atom C.[44] The unit cell of the inverse-Heusler-type alloys in the form of A_2BC with Hg_2CuTi type cubic structure and space group F43-m (No. 216); the Wyckoff positions (0, 0, 0), (1/2, 1/2, 1/2), (1/4, 1/4, 1/4) and (3/4, 3/4, 3/4) are occupied by A, B, A and C atoms, respectively. The crystal structure for Ru_2TGa alloy with (a) Cu_2MnAl-type and (b) Hg_2CuTi-type is illustrated in Fig. 1. In order to find the lattice constants of the equilibrium state of these alloys, the total energies (E) as a function of the unit cell volume (V_0) were calculated for the antiferromagnetic (AFM) and ferromagnetic (FM) states of both crystal structures. These variations of Ru_2CrGa, Ru_2MnGa, and Ru_2CoGa alloys are shown Fig. 2a, b and c, respectively. As can be seen from Fig. 2a, b and c, these alloys have smaller total energy values in the Cu_2MnAl-type structure than Hg_2CuTi-type structure. Thus, the Cu_2MnAl-type structure is energetically more suitable for the Ru_2TGa (T = Cr, Mn, and Co) Heusler alloys. Similarly, the AFM states are more suitable than other states in both crystal structures. The ground-state properties such as lattice constant (a_0), bulk modulus (B) and its pressure derivative (B') have been reckoned by fitting the total energy to the Murnaghan's equation of states.[38] These obtained outcomes for Ru_2TGa (T = Cr, Mn, and Co) alloys are tabulated along with the available experimental[23,24] and theoretical outcomes[26,29] in Table I. The equilibrium lattice constants were found to be 5.991 Å, 5.984 Å, and 5.936 Å for Ru_2TGa (T = Cr, Mn, and Co) alloys, respectively. These results are in good agreement with the results in the literature.[23,24,26,29] The bulk modulus for Ru_2TGa (T = Cr, Mn, and Co) alloys were found to be 238.1 GPa, 225.9 GPa, and 206.9 GPa, respectively. The calculated bulk modulus of these three alloys demonstrates the $Ru_2CoGa < Ru_2MnGa < Ru_2CrGa$ order. Since the atoms of Cr, Mn, and Co are in the same period, generally, the atomic radius decreases across the periods due to an increasing number of protons. The bulk modulus of Ru_2TGa (T = Cr, Mn, and Co) alloys decreases with decreasing atomic radius of the T atom, which is obviously seen from Table I. Similarly, the pressure derivatives of bulk modulus for Ru_2TGa (T = Cr, Mn, and Co) alloys also show the above sequence based on the displacement of the T (Cr, Mn, Co) atom.

The formation enthalpy (ΔH_f) is an important parameter for theoretically investigating structural stability and analyzing the probability of synthesis.[45,46] The formation enthalpy was calculated according to the following equation and given in Table I. The calculated formation enthalpies for these alloys agree well with the available results.[23,25,26,29]

$$\Delta H_f = E^{\text{total}}_{Ru_2TGa} - \left(2E^{\text{bulk}}_{Ru} + E^{\text{bulk}}_{T} + E^{\text{bulk}}_{Ga}\right) (\text{T} = \text{Cr, Mn, and Co}), \quad (1)$$

where $E^{\text{total}}_{Ru_2TGa}$ is the equilibrium total energy per formula unit of each alloy, E^{bulk}_{Ru}, E^{bulk}_{T}, and E^{bulk}_{Ga} are the energies per atom in Ru, T, and Ga stable bulk structures. The investigated Ru_2TGa (T = Cr, Mn, and Co) alloys have negative formation enthalpy. This indicates the structural stability of these alloys in the studied phase and thus these alloys are thermodynamically stable. As a result, these materials can be synthesized experimentally.

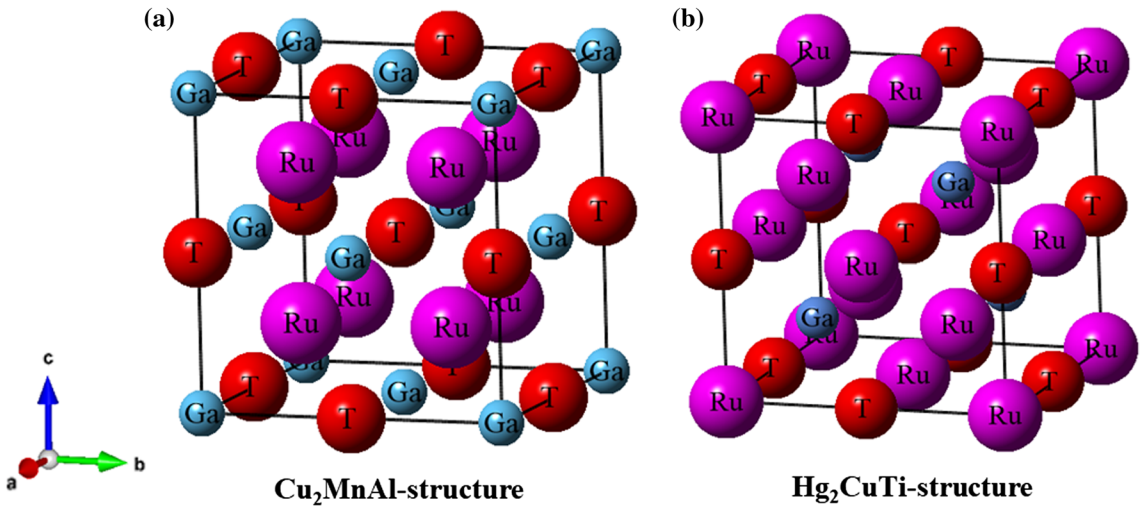

Fig. 1. (Color online) The crystal structure of the full-Heusler alloy Ru_2TGa (T = Cr, Mn, and Co) with (a) Cu_2MnAl-type and (b) Hg_2CuTi-type.

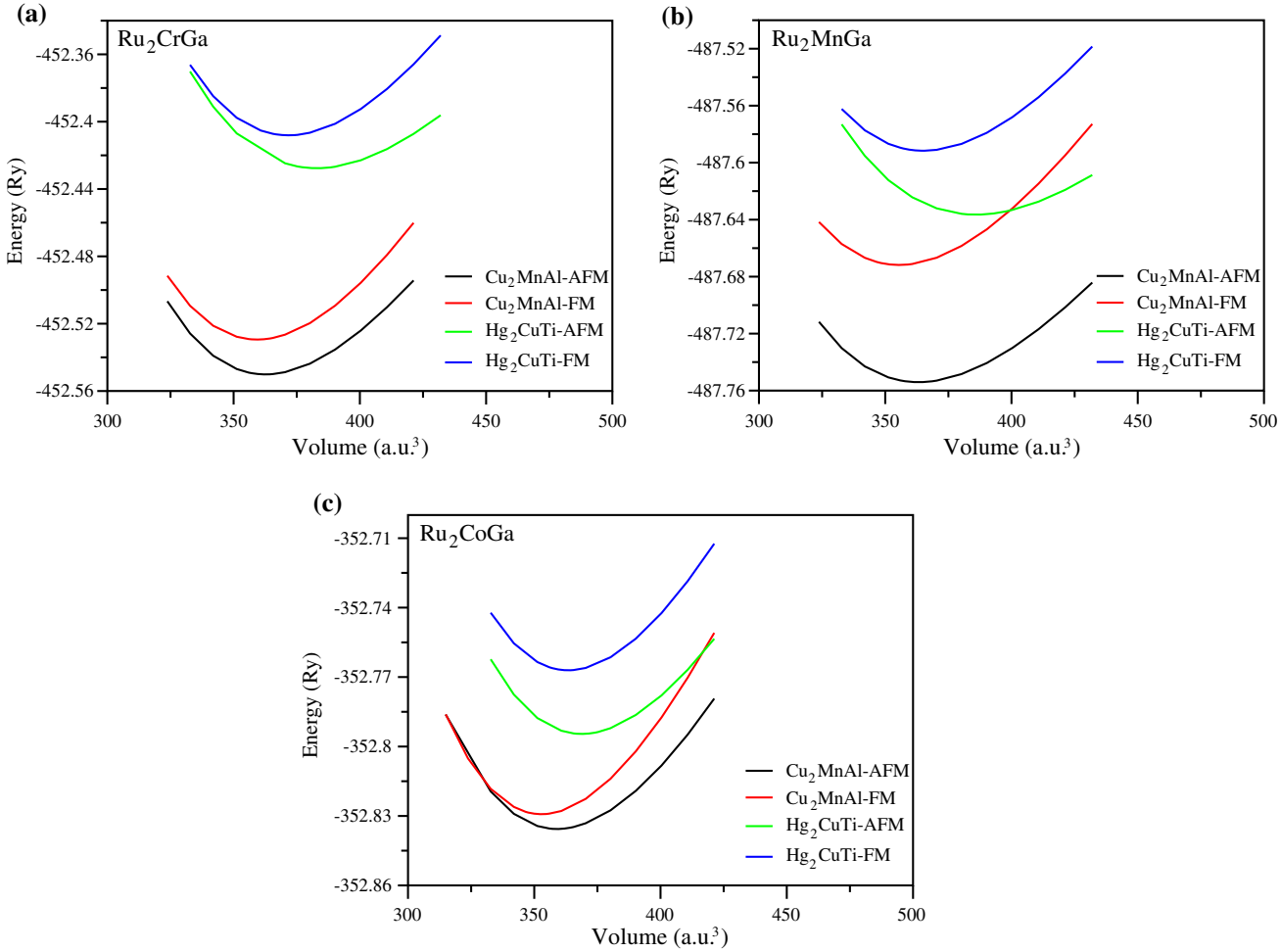

Fig. 2. (Color online) Total energy as a function of unit cell volume of the (a) Ru_2CrGa (b) Ru_2MnGa (c) Ru_2CoGa alloys for Cu_2MnAl-type and Hg_2CuTi-type structures in the antiferromagnetic (AFM) and ferromagnetic (FM) states.

Table I. Calculated lattice constant (a_0), Bulk modulus (B), pressure derivative of the Bulk modulus (B'), equilibrium lattice volumes (V_0) and formation enthalpy (ΔH_f) of Ru_2TGa (T = Cr, Mn, and Co) Heusler alloys

Material	Refs.	a_0 (Å)	B (GPa)	B' (GPa)	V_0 (a.u.^{3})	ΔH_f (kJ/mol)
Ru_2CrGa	Present	5.990	238.1	5.69	362.521	– 74.39
	Ref. 26	5.994	–	–	–	– 73.50
	Ref. 29	5.993	–	–	–	– 76.03
Ru_2MnGa	Present	5.993	225.9	5.55	363.113	– 96.68
	Refs. 23–Exp.	5.991	–	–	–	– 101.20
	Refs. 24–Exp.	5.992	–	–	–	–
	Refs. 25–Exp.	–	–	–	–	– 107.10
	Ref. 26	5.996	–	–		– 99.40
Ru_2CoGa	Present	5.971	206.9	4.75	359.097	– 24.60
	Ref. 26	5.940	–	–	–	– 20.80

Magnetic and Electronic Properties

Heusler alloys are of great importance because of their interesting and diverse magnetic properties such as ferromagnetism, antiferromagnetism, ferrimagnetism, paramagnetism and helimagnetism. For half-metallic materials, the Slater–Pauling rule[3,7] is a simple way of predicting the relation between the valence electron numbers and the total magnetic moment. It is well known that Heusler compounds generally conform to the following Slater–Pauling rule. This rule can help us to extrapolate their total magnetic moment.[47,48]

$$M_t = Z_T - 24 \quad (2)$$

Table II. Calculated total and partial spin magnetic moments (in μ_B) and the density of states at Fermi energy [$N\uparrow(E_F)$, $N\downarrow(E_F)$] and % spin polarization (P) of Ru_2TGa (T = Cr, Mn, and Co) Heusler alloys

Material	Refs.	M_t (μ_B)	$M_{Ru\ (1)}$ (μ_B)	$M_{Ru\ (2)}$ (μ_B)	M_T (μ_B)	M_{Ga} (μ_B)	$N\uparrow(E_F)$	$N\downarrow(E_F)$	P (%)
Ru_2CrGa	Present	1.16	− 0.264	− 0.264	1.718	− 0.028	2.53	0.19	86
	Ref. 26	1.14	–	–	–	–	–	–	–
	Ref. 29	1.5	0.0	–	1.5	0.0	–	–	–
Ru_2MnGa	Present	2.16	− 0.379	− 0.379	2.949	− 0.033	2.27	0.21	83
	Refs. 25–Exp.	2.18	–	–	–	–	–	–	–
	Ref. 26	2.15	–	–	–	–	–	–	–
Ru_2CoGa	Present	0.29	− 0.089	− 0.089	0.535	− 0.073	5.68	5.12	5
	Ref. 26	0.00	–	–	–	–	–	–	–

with M_t; the magnetic moment per formula unit and Z_T is the sum of the valence electron numbers of the atoms forming the alloy, or the sum of the number of spin-up and spin-down electrons. Total and partial spin magnetic moments of Ru_2TGa (T = Cr, Mn, and Co) Heusler alloys are listed together with available results in Table II. It is seen that the calculated total magnetic moments for Ru_2CrGa, Ru_2MnGa, and Ru_2CoGa alloys are 1.16 μ_B, 2.16 μ_B, and 0.29μ_B, respectively. Also, these values for three alloys are not integer numbers. Ru_2CrGa and Ru_2MnGa alloys indicate a small deviation from the Slater–Pauling behavior, whereas this deviation is larger for Ru_2CoGa alloy with a magnetic moment of 0.29 μ_B, and its electronic band structure represents metallic behavior in both spin states. The obtained total magnetic moments for these alloys are compatible with the previously reported values.[25,26,29] The total spin magnetic moment contains four contributions: the Ru (1) and Ru (2) atoms, the T (Cr, Mn, and Co) atom, the Ga atom. As seen from Table II, the major contribution to the total magnetic moment is mainly dominated by the T (Cr, Mn, Co) atom. It is due to the large exchange splitting between the spin-up and spin-down states of the T atom. The negative indication in the partial spin magnetic moments of Ru (1), Ru (2) and Ga atoms shows that the induced magnetic polarization of the Ru and Ga atoms is antiparallel to that of T atom. Also, the magnetic moment of the Ga atom is quite small. As a result, the partial magnetic moment of the Ga atom can be ignored on account of the absence of localized d electrons.

Spin-polarized electronic band structures along the high symmetry directions of Ru_2TGa (T = Cr, Mn, and Co) Heusler alloys for spin-up (majority-spin) and spin-down (minority-spin) states are illustrated in Fig. 3a, b and c, respectively. Fermi energy values have been subtracted from all energies and the Fermi energy level, indicated by dotted lines in the figures, is taken as zero. It is obviously seen that these alloys demonstrate metallic behavior owing to overlapping between conduction and valance bands at the Fermi level for both spin states. For better understanding of electronic contribution, the total and the partial density of states of Ru_2CrGa, Ru_2MnGa, and Ru_2CoGa alloys are plotted in Fig. 4a, b and c, respectively. The PDOS patterns for Ru_2CrGa and Ru_2MnGa alloys are very similar to each other. The Fermi level has vaguely contacted the maximum of valence states in the minority spin states. It is clear that the presence of minority spin states of Cr and Mn atoms at the Fermi level has completely destroyed the HM characteristic, and therefore Ru_2CrGa and Ru_2MnGa alloys are metallic. Besides, there is a small number of spin-down states at the bottom of the gap for Ru_2CrGa and Ru_2MnGa alloys. So this gap is just a pseudo-gap and shows that Ru_2CrGa and Ru_2MnGa alloys have not completed spin polarization. In addition to this, the total magnetic moment is not an integer. Such results have been observed in other Heusler alloys.[49] The lowest valence bands in the energy region that are lower than − 6 eV in both the majority and minority spin states mainly come from the electrons of 4s orbitals of the Ga atom and the electrons of 5p orbitals of the Ru atoms for all alloys. The low-energy part around − 6 eV and 0 eV in both spin states predominantly comes from the electrons of 4d orbitals of the Ru atom and the electrons of the 3d orbitals of the T (Cr, Mn, and Co) atom. Similarly, above the Fermi level, both the majority and minority spin states are dominated by Ru-4d orbitals and T (Cr, Mn, and Co)-3d orbitals. In addition, there is a strong hybridization between Ru-4d orbitals and T (Cr, Mn, and Co)-3d orbitals in both spin states.

Taking a closer look at the details of the density of states for each spin, we can define the term spin polarization, which is related to an imbalance in the spin density of states at the Fermi level. The following equation shows the traditional definition of spin polarization, which is the net spin present at the Fermi level described as a percentage:

$$P = \frac{N_\uparrow(E_F) - N_\downarrow(E_F)}{N_\uparrow(E_F) + N_\downarrow(E_F)} \times 100, \qquad (3)$$

where $N_\uparrow(E_F)$ and $N_\downarrow(E_F)$ are the density of states (DOS) for spin-up and spin-down electrons at the Fermi level. The calculated spin polarizations (P) of Ru_2TGa (T = Cr, Mn, and Co) alloys are listed in

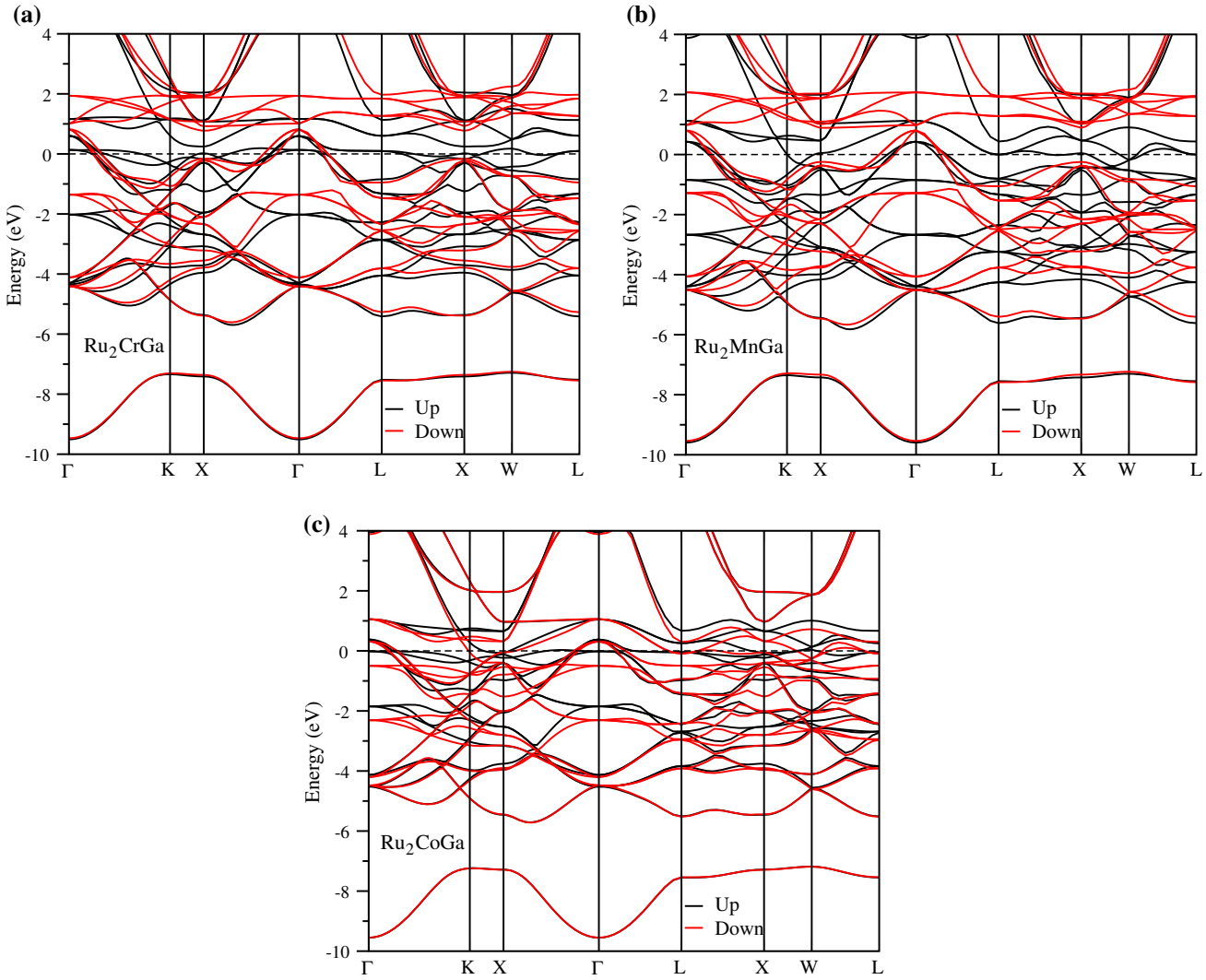

Fig. 3. (Color online) Electronic band structures in the spin-up (black line) and spin-down (red line) states of the (a) Ru_2CrGa (b) Ru_2MnGa (c) Ru_2CoGa alloys. The dotted line indicates the Fermi level at 0 eV.

Table II. According to Fig. 4a and b, the partial DOS of Ru_2CrGa and Ru_2MnGa alloys are very similar. In both Ru_2CrGa and Ru_2MnGa alloys, the Fermi level has vaguely contacted the maximum of valence states in the minority spin state and thus, the spin polarization has decreased from ideal 100% value to 86% and 83% values for Ru_2CrGa and Ru_2MnGa, respectively. Moreover, some of the Ru-based materials have been reported to exhibit antiferromagnetism.[50] In that case, the half-metallicity will be lost. The reason for the antiferromagnetic ground state may be found in on-site correlation at the Mn atoms, which was not included here.

Elastic Properties

Elastic constants are important parameters for characterizing solid materials. They usually contain significant information about a material's structural and mechanical stability, and are closely related to physical properties such as Debye temperature, melting point, specific heat and thermal expansion coefficient. Calculated elastic constants (C_{11}, C_{12} and C_{44}) of Ru_2TGa (T = Cr, Mn, and Co) alloys have been tabulated in Table III. Ru_2TGa (T = Cr, Mn, and Co) Heusler alloys with Fm-3m crystal symmetry have three independent second-order elastic constants such as C_{11}, C_{12} and C_{44} since they are cubic. Mechanical stability conditions of elastic constants in cubic crystals are given in the following equations[51,52]:

$$C_{11} > 0, C_{11} - C_{12} > 0, \\ C_{11} + 2C_{12} > 0, C_{44} > 0 \text{ and } C_{12} < B < C_{11} \quad (4)$$

In view of these stability conditions, it is understood from Table III that these alloys are mechanically stable in the $L2_1$ cubic phase. From these

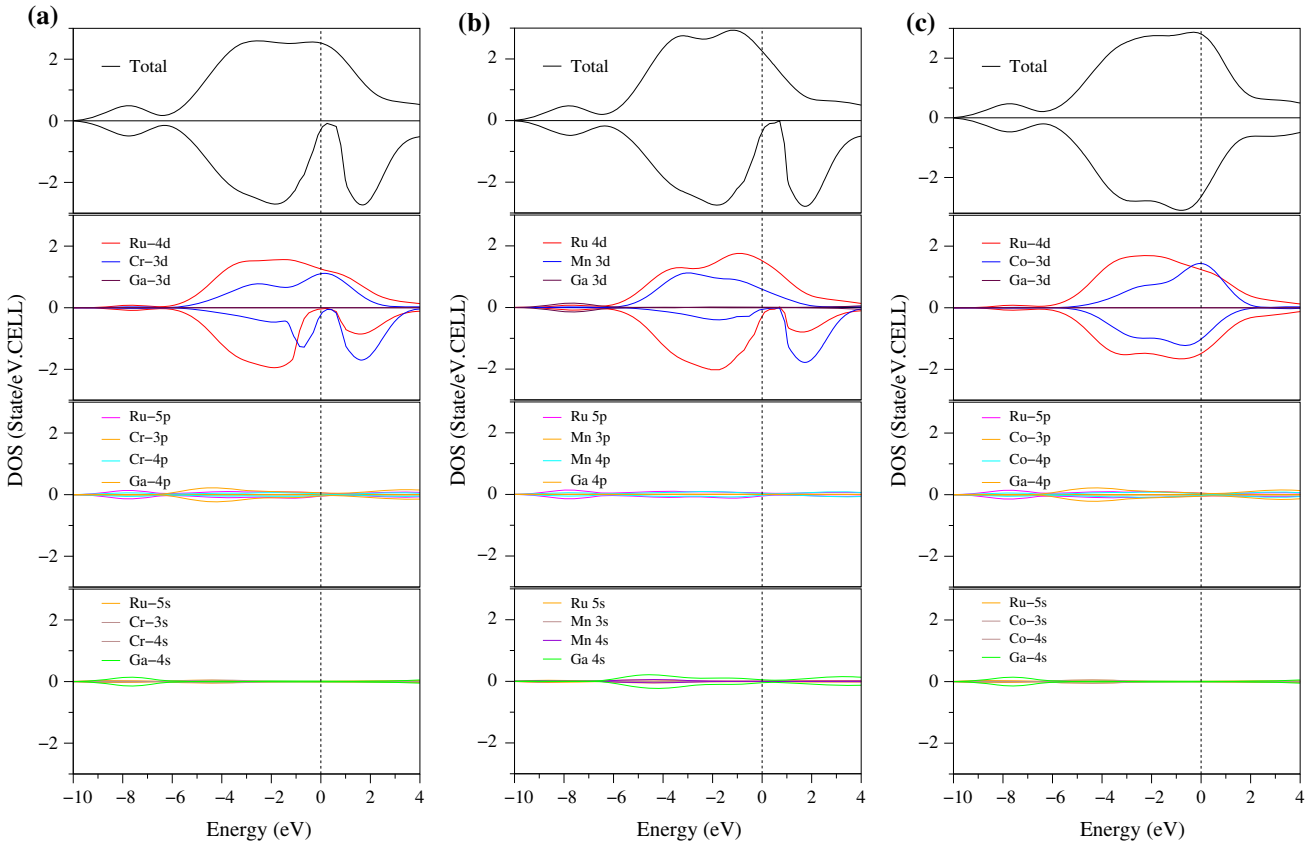

Fig. 4. (Color online) Spin-polarized DOS and PDOS of the (a) Ru_2CrGa (b) Ru_2MnGa (c) Ru_2CoGa alloys. The dotted line indicates the Fermi level at 0 eV.

Table III. Calculated elastic constants (C_{ij}), Bulk modulus (B), Shear modulus (G, G_V, *and* G_R), the ratio of B/G, Young's modulus (E), Poisson ratio (v) and Vickers hardness (H_V) of Ru_2TGa (T = Cr, Mn, and Co) alloys

Material	C_{11} (GPa)	C_{12} (GPa)	C_{44} (GPa)	B (GPa)	G_V (GPa)	G_R (GPa)	G (GPa)	B/G	E (GPa)	v	H_V (GPa)
Ru_2CrGa	379.09	174.79	122.49	242.89	114.35	113.45	113.90	2.13	295.52	0.297	10.16
Ru_2MnGa	357.37	166.25	166.67	229.96	138.23	128.44	133.34	1.73	335.22	0.257	15.49
Ru_2CoGa	428.36	107.09	125.60	214.18	139.61	137.60	138.61	1.55	342.04	0.234	18.52

elastic constants (C_{11}, C_{12} and C_{44}), the mechanical parameters of the Ru_2TGa (T = Cr, Mn, and Co) Heusler alloys can be obtained using the Voigt–Reuss–Hill approximation.[53–55] The mechanical parameters such as bulk modulus (B), shear modulus (G), Voigt (G_V) and Reuss (G_R) polycrystalline elastic modulus, B/G ratio, Young's modulus (E), Poisson's ratio (v), and Vickers hardness (H_V) are computed from the following equations; the results are given in Table III.

$$G_V = \frac{1}{5}(C_{11} - C_{12} + 3C_{44}) \tag{5}$$

$$G_R = \frac{5C_{44}(C_{11} - C_{12})}{4C_{44} + 3(C_{11} - C_{12})} \tag{6}$$

$$G_H = G = \frac{1}{2}(G_V + G_R) \tag{7}$$

$$E = \frac{9BG}{(3B + G)} \tag{8}$$

$$v = \frac{1}{2}\left[\frac{B - \frac{2}{3}G}{B + \frac{1}{3}G}\right] \tag{9}$$

$$H_V = 2\left(k^2G\right)^{0.585} - 3; (k = G/B) \tag{10}$$

here, the G_V is the Voigt shear modulus corresponding to the upper limit of the G, and the G_R is the

Reuss shear modulus corresponding to the lower limit of the G. The shear modulus (G), which is a measure of its resistance to reversible deformations, is one of the most important parameters that describe the hardness of a material. The obtained shear modulus (G), Voigt (G_V) and Reuss (G_R) polycrystalline elastic modulus of these three alloys are in the sequence $Ru_2CrGa < Ru_2MnGa < Ru_2CoGa$. This result shows that the G, G_V and G_R values increase while going from Ru_2CrGa to Ru_2CoGa.

The bulk modulus (B) is defined as a measure of the energy required to create a deformation. The values for Ru_2TGa (T = Cr, Mn, and Co) alloys are calculated as 242.89 GPa, 229.96 GPa, and 214.18 GPa, respectively. It is clear that the bulk modulus derived from the calculated elastic constants for Ru_2TGa (T = Cr, Mn, Co) alloys decreases when the T atom goes from Cr to Co. It is evident that bulk modulus of Ru_2TGa (T = Cr, Mn, and Co) decreases as T atom goes from Cr to Co. Bulk modulus values derived from elastic constants and those obtained by using the Murnaghan equation are highly compatible with each other.

Pugh's B/G ratio[56] is one of the criteria commonly used to provide information about the fragility (ductile nature) of materials. According to this criterion, if this value is smaller than 1.75, the material is fragile; if it is the larger it is ductile. From the B/G ratios calculated for these alloys, the Ru_2MnGa (1.73) and Ru_2CoGa (1.55) alloys are brittle because their ratios are smaller than 1.75. On the contrary the Ru_2CrGa (2.13) alloy is ductile because its ratio greater than 1.75. At the same time, the B/G ratio is also a measure for the hardness of materials. Generally, a material having a low B/G ratio has a high hardness. We would expect that the Ru_2CoGa alloy is harder than the others. Young's modulus (E) is a measure of hardness; the greater the E value, the harder the material. According to the calculated Young's modulus values for these materials, the hardness order is $Ru_2CoGa > Ru_2MnGa > Ru_2CrGa$. That is, E increases when going from Ru_2CrGa to Ru_2CoGa.

Poisson's ratio (v) is not only a measure of the compressibility of a material, but also an indication of the characteristics of its bonding forces.[57] If Poisson's ratio is in the range of 0.25–0.5,[58] the materials are more stable under exterior degradation and less compressible, while outside of this range, the materials become much more compressible. From Table III, it may be readily viewed that the Ru_2CrGa and Ru_2MnGa full-Heusler alloys are less compressible due to their Poisson's ratios in this range. On the other hand, since the Poisson's ratio of the Ru_2CoGa alloy is outside this range, it is more compressible. In addition, Poisson's ratio reveals information about the bond forces of the material. The value of Poisson's ratio (v) is close to 0.1 for covalent materials and 0.25 for ionic materials.[59] It can be said that these alloys have an ionic character, since the Poisson's ratios in Table III are 0.297, 0.257 and 0.234. As clearly seen from Table III, Poisson's ratios of these alloys decrease with decreasing the atomic radius of the T (Cr, Mn, Co) atom.

The Vickers hardness (H_V) of a material is directly related to other mechanical properties. Hardness is a relative measure defined as the resistance of the materials against scratching, cutting, corrosion and perforation.[46] If the hardness of a material is smaller than 10 GPa, the material is soft; if it is between 10 GPa and 40 GPa, the material is hard; if it is greater than 40 GPa, it is considered to be a very hard material.[60–62] There are theoretically many different methods for determining hardness. One of them is the quasi-experimental method given by Eq. 10, which is in relation to the bulk and shear modulus developed by Chen et al.[63] Based on calculated hardness values, all the alloys studied here can be defined as hard materials since their Vickers hardness values are greater than the critical value of 10 GPa. Among the studied alloys, Ru_2CoGa has the greatest hardness.

Elastic Anisotropy

Materials whose physical properties vary according to direction are called anisotropic materials.[46] This is due to the different atomic densities in the crystal directions. The shear anisotropy factor is a measure of the degree of elastic anisotropy. If the value of the anisotropy factor is 1, the material is elastically isotropic, otherwise, the material is anisotropic. For a cubic structure, the anisotropy factor can be expressed in terms of elastic constants as follows[64,65]:

$$A_1 = A_2 = A_3 = A = \frac{2C_{44}}{(C_{11} - C_{12})} \tag{11}$$

The universal elastic anisotropy index (A^U) and elastic anisotropy percentages (A_B,A_G) of bulk modulus and shear modulus have been computed by means of the equations given below.[66]

$$A^U = 5\frac{G_V}{G_R} + \frac{B_V}{B_R} - 6 \geq 0 \tag{12}$$

$$A_B = \frac{B_V - B_R}{B_V + B_R} \times 100\% \tag{13}$$

$$A_G = \frac{G_V - G_R}{G_V + G_R} \times 100\% \tag{14}$$

The A, A^U, A_B and A_G values of Ru_2TGa (T = Cr, Mn, and Co) alloys were calculated; results are given in Table IV. The fact that the anisotropy factors differ from 1 indicates that these alloys are anisotropic. When these alloys are sorted according to the degree of anisotropy, the sequence is $Ru_2MnGa > Ru_2CrGa > Ru_2CoGa$. Namely, Ru_2MnGa

Table IV. Calculated shear anisotropic factor (A), the percentage (in %) of anisotropy in the compression and shear (A_B and A_G), and the universal anisotropic index (A^U) of Ru_2TGa (T = Cr, Mn, and Co) Heusler alloys

Material	A	A_B(%)	A_G (%)	A^U
Ru_2CrGa	1.20	0	0.40	0.04
Ru_2MnGa	1.74	0	3.37	0.38
Ru_2CoGa	0.78	0	0.73	0.07

has the largest anisotropy. As seen from Table IV, since the elastic anisotropy index (A^U) is different from 0, all alloys are anisotropic. The Ru_2MnGa alloy has much more anisotropy than other alloys. This is consistent with the results obtained from anisotropy factors.

The directional dependencies of Young's modulus, linear compressibility, shear modulus, and Poisson's ratio for these alloys have been investigated via the EIAM software.[67] The obtained parameters for Ru_2CrGa, Ru_2MnGa, and Ru_2CoGa full-Heusler alloys have been given with both 2D and 3D presentations in Figs. 5, 6, and 7, respectively. The deviations from the spherical shape in the figures of these physical properties show the degree of anisotropy. In Figs. 5, 6 and 7, the blue curves represent the maximum values and the green curves represent the minimum values for the parameters. The maximum and minimum values of Young's modulus (E), linear compressibility (β), shear modulus (G) and Poisson's ratio (υ) for these alloys are also listed in Table V. As we can clearly see from Figs. 5b, 6b, 7b, the 3D presentations of the linear compressibility for these alloys have nearly spherical structure, which indicates that the linear compressibility of every alloy is only very slightly anisotropic. For the cubic Ru_2MnGa with the largest A_G (3.37) and A^U (0.38), the 3D figures of Young's modulus, shear modulus, and Poisson's ratio have openly deviated in shape from the sphere. In other words, this alloy has the most powerful anisotropy for different orientations. It can be concluded from the 3D directional dependences of Young's modulus, shear modulus, and Poisson's ratio, that the extent of the elastic anisotropy for these alloys follows the order of Ru_2MnGa > Ru_2CrGa > Ru_2CoGa. This result is coherent with the results obtained from the survey of the universal elastic anisotropy index and elastic anisotropy percentages.

Vibrational and Thermodynamical Properties

Phonon dispersion curves are necessary for the microscopic understanding of the lattice dynamics. The phonon dispersion curves calculated along the high symmetry directions, total and partial density of states (DOS) for Ru_2CrGa, Ru_2MnGa, and Ru_2CoGa Heusler alloys are plotted in Fig. 8a, b and c, respectively. Since there are four atoms in the primitive cell of these alloys, there are totally twelve branches in the phonon dispersion curves, consisting of three acoustic and nine optical branches. Ru_2TGa (T = Cr, Mn, and Co) alloys are dynamically stable, since negative mode is not observed in the phonon dispersion curves. Since the mass difference between the Ru, T and Ga atoms was small, no gap was observed between the acoustic modes and optical modes in the phonon dispersion curves. The frequencies of optical phonon modes at the Γ point are 6.508 THz, 6.957 THz and 7.393 THz for Ru_2CrGa; 6.700 THz, 6.919 THz and 7.701 THz for Ru_2MnGa; and 5.729 THz, 6.314 THz and 6.964 THz for Ru_2CoGa, respectively. Interaction between some optical modes and acoustic modes was observed at frequencies below about 4 THz. Since optical modes play an important role in carrying thermal conductivity, this interaction causes a decrease in thermal conductivity.[68] This interaction is more, in particular, in the Ru_2CoGa alloy, so the thermal conductivity of this alloy is expected to be lower. This result is consistent with the Debye temperatures given in Table VI. When we look at the phonon DOS curves of these alloys, it is seen that every three atoms forming these alloys are also vibrating in acoustical and optical regions. Phonon dispersion results at the Γ point of these alloys may provide beneficial knowledge for future experiments in order to specify new phases.

It is known that the first-principles phonon calculations are limited for the thermodynamic properties of the crystals, but these properties can be determined in detail by phonons.[69] The specific heat capacity and entropy as a function of temperature can be described with the quasi-harmonic approximation. The temperature dependence of heat capacity and entropy for these alloys are given in Fig. 9a and b, respectively. The thermal properties are determined in the temperature range from 0 K to 1000 K for Ru_2TGa (T = Cr, Mn, and Co) alloys, where the quasi-harmonic model remains fully valid. As the temperature rises, the heat capacity increases quickly up to nearly 350 K; after this temperature, it goes up at a smaller rate. This correlation is consistent with the Debye temperatures as given in Table - VI. The heat capacity arrives at a steady value named as the Dulong-Petit limit at high temperatures about 700 K. The entropy curves exhibit the expected behavior at the considered temperature range. Because of the vibrational contribution, the entropy curves increase rapidly as temperature increases. The increasing rate is relatively slower for Ru_2CrGa and Ru_2MnGa compared to Ru_2CoGa.

Debye temperature (Θ_D) is a basic physical property associated with specific heat, elastic constants, and melting temperature. It is used to distinguish between low and high-temperature zones in a material. The material with a high Debye

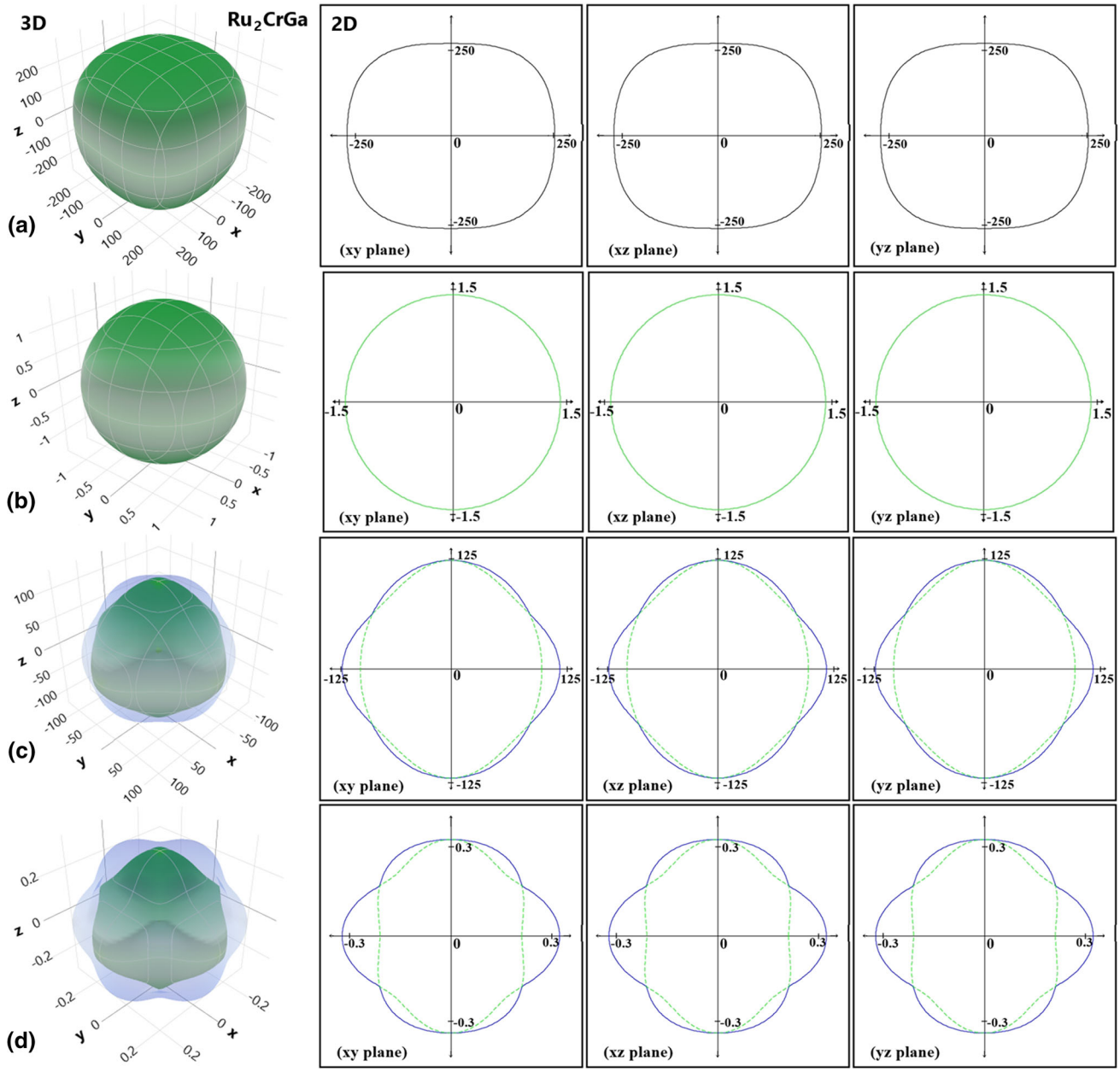

Fig. 5. (Color online) Calculated directional dependence of the mechanical properties; (a) Young's modulus, (b) linear compressibility, (c) shear Modulus, (d) Poisson's ratio for Ru_2CrGa.

temperature has a higher thermal conductivity. The calculated densities (ρ), the longitudinal, transverse and average sound velocities (v_l, v_t, and v_m), and the Debye temperatures (Θ_D) of these alloys are given in Table VI. The order of Debye temperatures, which may be deduced from Table VI, is $Ru_2MnGa > Ru_2CrGa > Ru_2CoGa$. That is, the material with the highest Debye temperature is Ru_2MnGa and the lowest is Ru_2CoGa. Therefore, the thermal conductivity of the Ru_2MnGa alloy is higher than the others. In this study, the Debye temperatures of Ru_2TGa (T = Cr, Mn, and Co) alloys have been determined via the following equation[70]:

$$\Theta_D = \frac{h}{k}\left[\frac{3n}{4\pi}\left(\frac{N_A\rho}{M}\right)\right]^{1/3} v_m, \tag{15}$$

where h is Planck's constant, k is Boltzmann's constant, n is the total number of atoms in the molecule, N_A is Avogadro's number, ρ is the density, M is the molecular weight and v_m is the average sound velocity. The v_m value of the Ru_2TGa (T = Cr, Mn, and Co) Heusler alloys is derived from the following equations[71]:

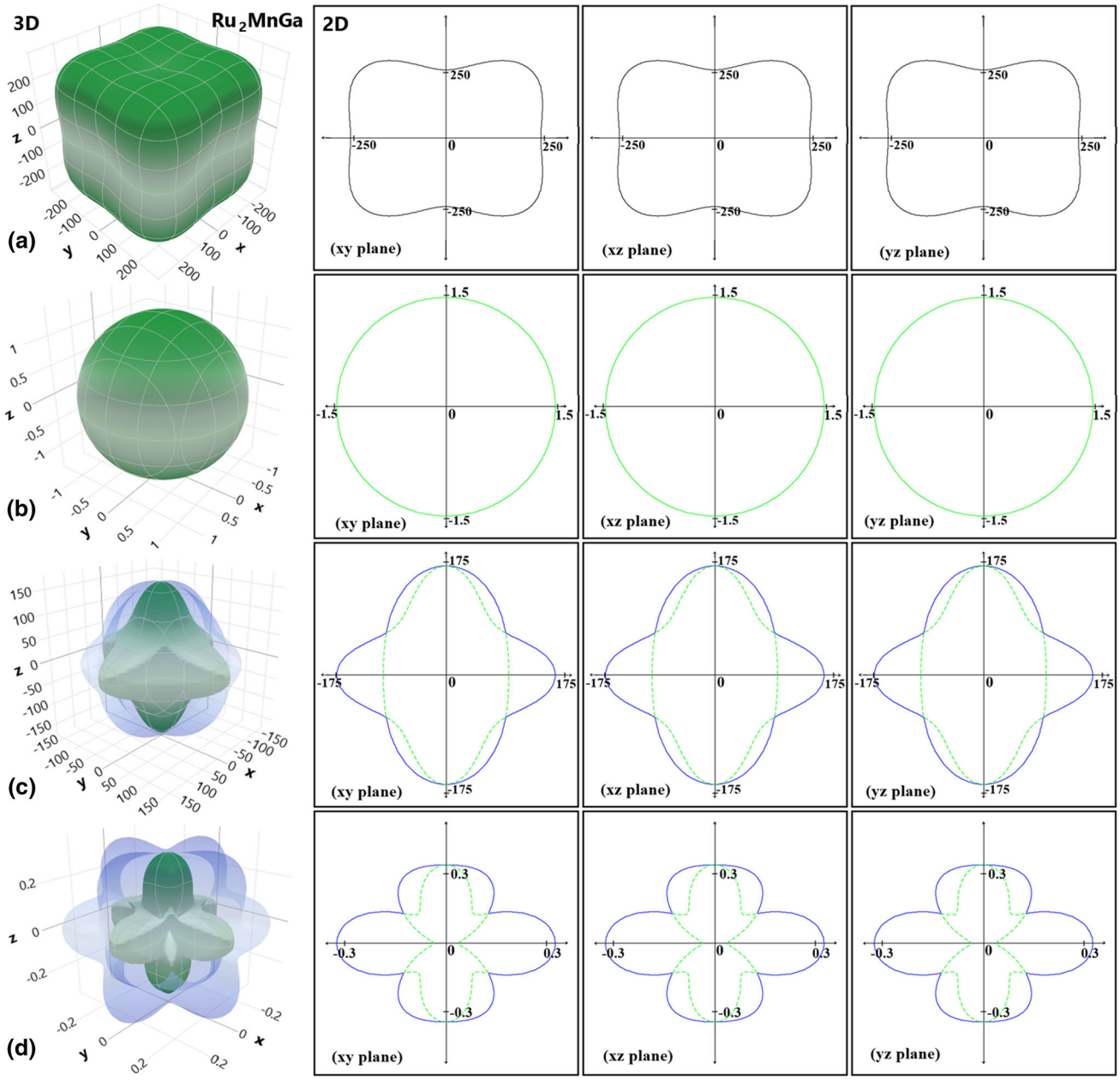

Fig. 6. (Color online) Calculated directional dependence of the mechanical properties; (a) Young's modulus, (b) linear compressibility, (c) shear Modulus, (d) Poisson's ratio for Ru_2MnGa.

$$v_m = \left[\frac{1}{3}\left(\frac{2}{v_t^3}+\frac{1}{v_l^3}\right)\right]^{-1/3}; v_l = \sqrt{\frac{3B+4G}{3\rho}}; v_t = \sqrt{\frac{G}{\rho}} \tag{16}$$

where v_l and v_t are longitudinal and transverse sound velocities which are obtained by means of Navier equations.[72] Moreover, the melting temperature (T_{melt}) is obtained using the following relation[73] and its values are given in Table VI.

$$T_{\text{melt}} = \left[553 + \left(\frac{5.91C_{11}}{\text{GPa}}\right)\right]K \mp 300\ \text{K} \tag{17}$$

It is found that the melting point of Ru_2CoGa is higher than those of others. This conclusion is in concordance with what I interpreted in results for Young's modulus, that Ru_2CoGa is harder than Ru_2CrGa and Ru_2MnGa alloys. As far as I know, there are no available experimental or theoretical

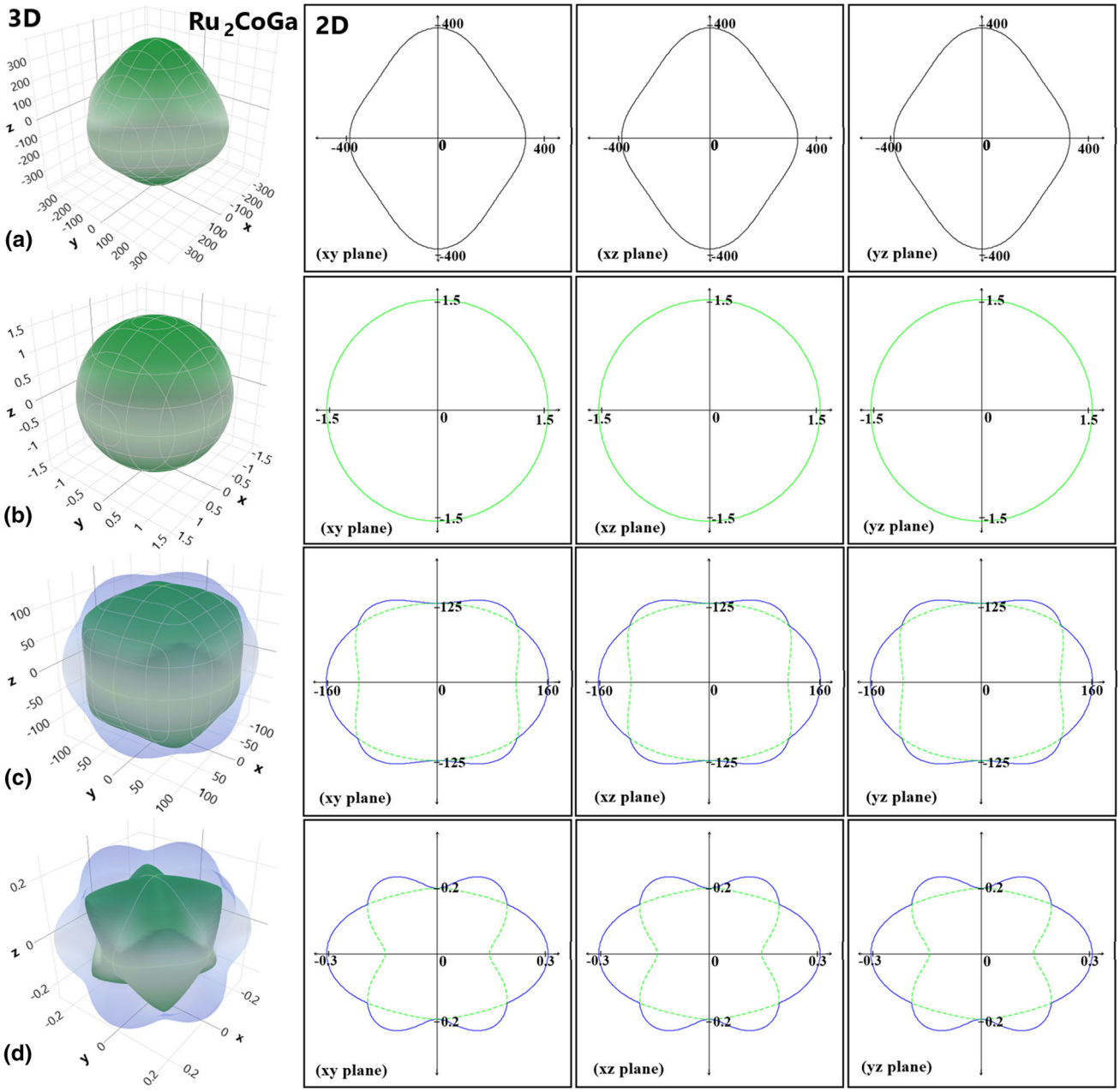

Fig. 7. (Color online) Calculated directional dependence of the mechanical properties; (a) Young's modulus, (b) linear compressibility, (c) shear Modulus, (d) Poisson's ratio for Ru_2CoGa.

Table V. The maximum and minimum values of Young's modulus (E, in GPa), linear compressibility (β, in TPa^{-1}), shear modulus (G, in GPa) and Poisson's ratio (v) of Ru_2TGa (T = Cr, Mn, and Co) Heusler alloys

	Young's modulus		Linear compressibility		Shear modulus		Poisson's ratio	
Material	E_{min}	E_{max}	β_{min}	β_{max}	G_{min}	G_{max}	v_{min}	v_{max}
Ru_2CrGa	268.77	314.59	1.37	1.37	102.15	122.49	0.23	0.35
Ru_2MnGa	251.8	402.72	1.45	1.45	95.56	166.67	0.05	0.44
Ru_2CoGa	315.19	385.52	1.56	1.56	125.6	160.63	0.17	0.32

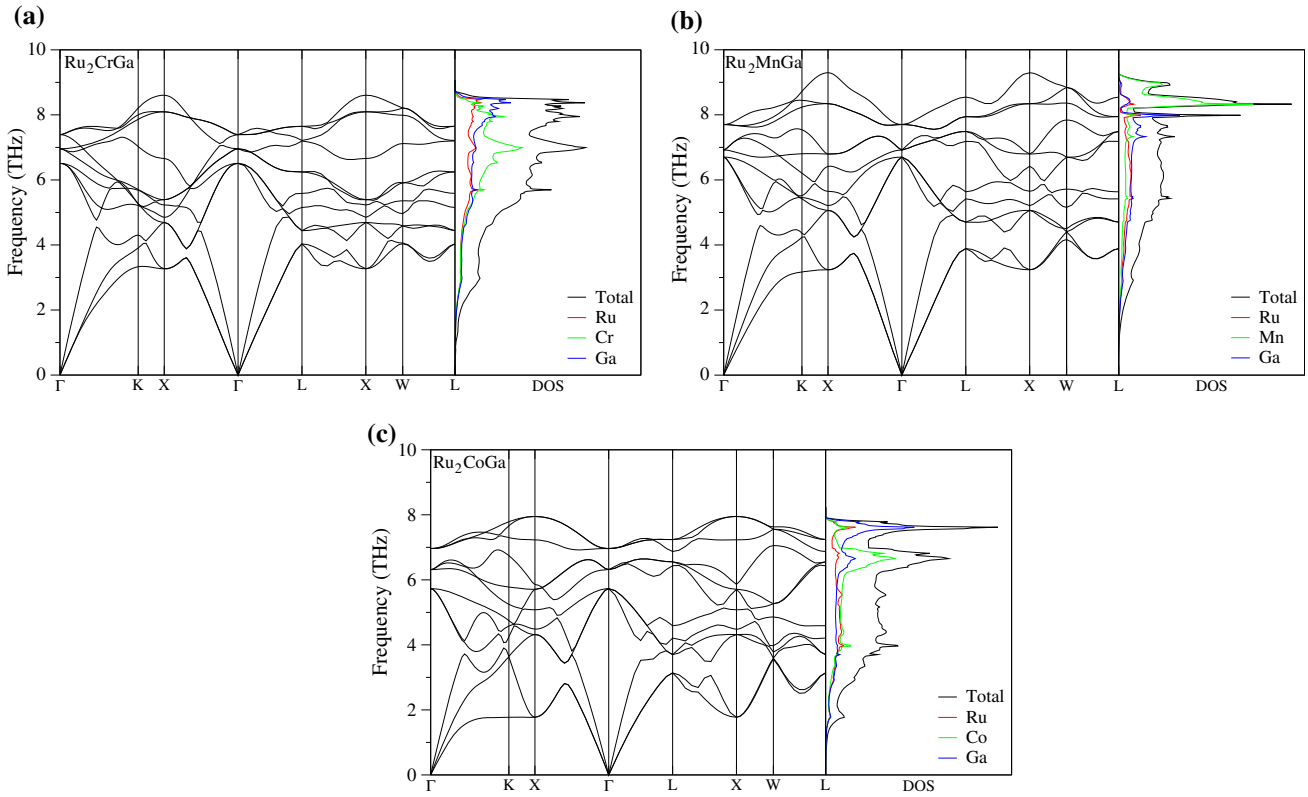

Fig. 8. (Color online) Calculated phonon dispersion curves and phonon DOS for (a) Ru_2CrGa (b) Ru_2MnGa (c) Ru_2CoGa alloys.

Table VI. The calculated density (ρ in g cm^{-3}), the longitudinal, transverse and average sound velocity (v_l, v_t, and v_m; in m s^{-1}), the Debye temperature (Θ_D) and the melting temperature (T_{melt}) of Ru_2TGa (T = Cr, Mn, and Co) Heusler alloys

Material	ρ	v_l (m/s)	v_t (m/s)	v_m (m/s)	Θ_D(K)	$T_{melt}(K)$
Ru_2CrGa	10.032	6273	3370	3762	361.61	2793.42 ± 300
Ru_2MnGa	10.128	6345	3628	4032	378.86	2665.06 ± 300
Ru_2CoGa	10.504	6163	3633	4025	330.30	3084.61 ± 300

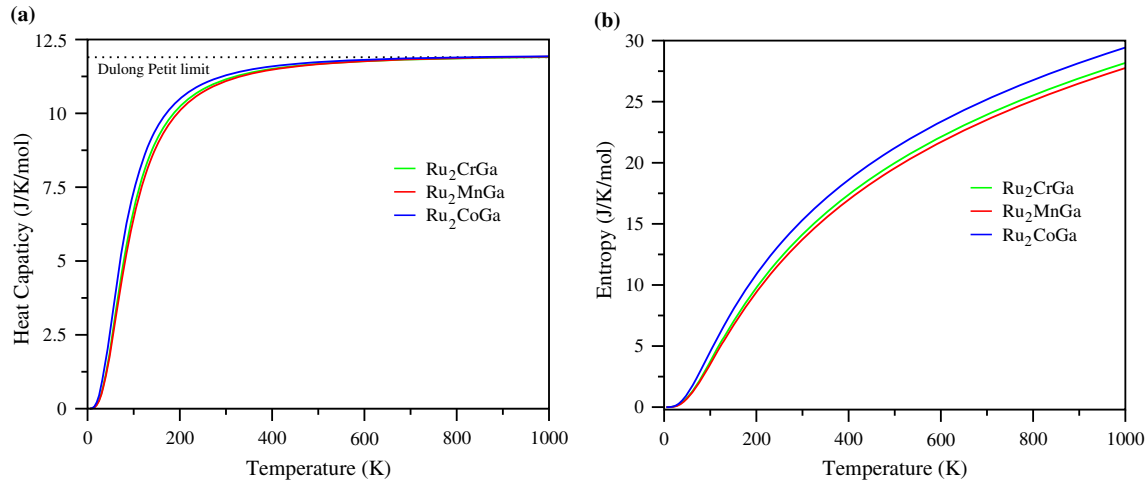

Fig. 9. (Color online) The temperature dependence of heat capacity (a) and entropy (b) for Ru_2TGa (T = Cr, Mn, and Co) alloys.

results associated with vibrational and thermodynamic properties in the literature with which to compare our results.

CONCLUSIONS

The magnetic, electronic, mechanic, anisotropic elastic and vibrational properties of Ru_2TGa (T = Cr, Mn, and Co) Heusler alloys were comprehensively studied by first-principles methods using the GGA-PBE. It has been found that the antiferromagnetic state in the Cu_2MnAl-type structure is energetically more stable than other states. The obtained structural parameters are in good agreement with both experimental and theoretical results in the literature. Band structure calculations show that each alloy has a metallic character in nature. Besides, the spin-down states of the other two alloys except for Ru_2CoGa have a pseudo-gap at the Fermi level. For this reason, the spin polarization has decreased from the ideal 100% value to 86% and 83% for Ru_2CrGa and Ru_2MnGa, respectively. On the other hand, the total magnetic moments of these alloys are 1.16%, 2.16% and 0.29% μ_B, respectively. The total spin magnetic moments of Ru_2TGa (T = Cr, Mn, and Co) alloys mainly originate from the T atom. Moreover, Ru_2MnGa and Ru_2CoGa alloys exhibit brittleness, where Ru_2CrGa alloy exhibits ductility. Elastic parameters, including bulk modulus (B), shear modulus (G), Voigt (G_V) and Reuss (G_R) polycrystalline elastic modulus, B/G ratio, Young's modulus (E), Poisson's ratio (υ), and Vickers hardness (H_V) were specified and discussed. The predicted anisotropy factors were investigated in detail. All the alloys in this study show mostly mechanical anisotropy. The obtained results show that the Ru_2TGa (T = Cr, Mn, and Co) Heusler alloys are both mechanically and dynamically stable in the studied phase. It is anticipated that the given results might trigger future experimental studies of Ru-based Heusler alloys.

REFERENCES

1. F. Heusler, *Verh. Dtsch. Phys. Ges.* 5, 219 (1903).
2. S. Khmelevskyi, E. Simon, L. Szunyogh, and P. Mohn, *J. Alloys Compd.* 692, 178 (2017).
3. I. Galanakis, P.H. Dederichs, and N. Papanikolaou, *Phys. Rev. B* 66, 174429 (2002).
4. S.D. Bader and S.S.P. Parkin, *Annu. Rev. Condens. Matter Phys.* 1, 71 (2010).
5. R.A. De Groot, F.M. Mueller, P.G. Van Engen, and K.H.J. Buschow, *Phys. Rev. Lett.* 50, 2024 (1983).
6. I. Žutić, J. Fabian, and S.D. Sarma, *Rev. Mod. Phys.* 76, 323 (2004).
7. I. Galanakis, P. Mavropoulos, and P.H. Dederichs, *J. Phys. D Appl. Phys.* 39, 765 (2006).
8. Z. Charifi, H. Baaziz, S. Noui, Ş. Uğur, G. Uğur, A. Iyigör, A. Candan, and Y. Al-Douri, *Comput. Mater. Sci.* 87, 187 (2014).
9. E. Şaşıoğlu, L.M. Sandratskii, and P. Bruno, *Phys. Rev. B* 70, 024427 (2004).
10. J. Kübler, G.H. Fecher, and C. Felser, *Phys. Rev. B* 76, 024414 (2007).
11. F. Hajizadeh and F. Ahmadian, *J. Supercond. Nov. Magn.* 31, 3515 (2018).
12. P. Entel, V.D. Buchelnikov, V.V. Khovailo, A.T. Zayak, W.A. Adeagbo, M.E. Gruner, H.C. Herper, and E.F. Wassermann, *J. Phys. D Appl. Phys.* 39, 865 (2006).
13. A. Ayuela, J. Enkovaara, K. Ullakko, and R.M. Nieminen, *J. Phys. Condens. Matter* 11, 2017 (1999).
14. M. Sargolzaei, M. Richter, K. Koepernik, I. Opahle, H. Eschrig, and I. Chaplygin, *Phys. Rev. B* 74, 224410 (2006).
15. C.S. Jiang, W. Peng, C. Liu, X. Deng, J. Yuan, and Y. Wen, *J. Magn. Magn. Mater.* 471, 82 (2019).
16. A. Erkisi, G. Surucu, and R. Ellialtioglu, *Philos. Mag.* 97, 2237 (2017).
17. F. Dahmane, Y. Mogulkoc, B. Doumi, A. Tadjer, R. Khenata, S.B. Omran, D.P. Rai, G. Murtaza, and D. Varshney, *J. Magn. Magn. Mater.* 407, 167 (2016).
18. R. Haleoot and B. Hamad, *J. Elect. Mat.* 48, 1164 (2019).
19. A. Candan, G. Uğur, Z. Charifi, H. Baaziz, and M.R. Ellialtıoğlu, *J. Alloys Compd.* 560, 215 (2013).
20. S. Noui, Z. Charifi, H. Baaziz, G. Uğur, and Ş. Uğur, *J. Elect. Mat.* 48, 337 (2019).
21. S.A. Khandy, I. Islam, D.C. Gupta, R. Khenata, and A. Laref, *Sci. Rep.* 9, 1475 (2019).
22. P.D. Patel, S. Shinde, S.D. Gupta, and P.K. Jha, *J. Elect. Mat.* 48, 1634 (2019).
23. M. Yin and P. Nash, *J. Alloys Compd.* 634, 70 (2015).
24. T. Hori, M. Akimitsu, H. Miki, K. Ohoyoama, and Y. Yamaguchi, *Appl. Phys. A* 74, 737 (2002).
25. M. Žic, K. Rode, N. Thiyagarajah, Y.C. Lau, D. Betto, J.M.D. Coey, S. Sanvito, K.J. O'Shea, C.A. Ferguson, D.A. MacLaren, and T. Archer, *Phys. Rev. B* 93, 140202 (2016).
26. M. Gilleßen, and R. Dronskowski, Maßgeschneidertes und Analytik-Ersatz über die quantenchemischen Untersuchungen einiger ternärer intermetallischer Verbindungen (No. RWTH-CONV-113777), *Fachgruppe Chemie* (2010).
27. S.V. Faleev, Y. Ferrante, J. Jeong, M.G. Samant, B. Jones, and S.S. Parkin, *Phys. Rev. B* 95, 045140 (2017).
28. S.V. Faleev, Y. Ferrante, J. Jeong, M.G. Samant, B. Jones, and S.S. Parkin, *Phys. Rev. Appl.* 7, 034022 (2017).
29. J. Balluff, Ph. D. thesis, Ab initio to application antiferromagnetic Heusler compounds for spintronics (2017).
30. J. Balluff, K. Diekmann, G. Reiss, and M. Meinert, *Phys. Rev. Mat.* 1, 034404 (2017).
31. D. Vanderbilt, *Phys. Rev. B* 41, 7892 (1990).
32. J.P. Perdew, J.A. Chevary, S.H. Vosko, K.A. Jackson, M.R. Pederson, D.J. Singh, and C. Fiolhais, *Phys. Rev. B* 46, 6671 (1992).
33. Y. Zhang and W. Yang, *Phys. Rev. Lett.* 80, 890 (1998).
34. J.P. Perdew, K. Burke, and M. Ernzerhof, *Phys. Rev. Lett.* 77, 3865 (1996).
35. P. Giannozzi, S. Baroni, N. Bonini, M. Calandra, R. Car, C. Cavazzoni, D. Ceresoli, G. L. Chiarotti, M. Cococcioni, I. Dabo, A. D. Corso, S. Gironcoli, S. Fabris, G. Fratesi, R. Gebauer, U. Gerstmann, C. Gougoussis, A. Kokalj, M. Lazzeri, L. M. Samos, N. Marzari, F. Mauri, R. Mazzarello, S. Paolini, A. Pasquarello, L. Paulatto, C. Sbraccia, S. Scandolo, G. Sclauzero, A. P. Seitsonen, A. Smogunov, P. Umari, and R. M. Wentzcovitch, *J. Phys. Conden. Matter.* 21, 395502 (2009).
36. P. Hohenberg and W. Kohn, *Phys. Rev. B* 136, 864 (1964).
37. W. Kohn and L. Sham, *J. Phys. Rev. A* 140, 1133 (1965).
38. F.D. Murnaghan, *Proc. Natl. Acad. Sci. U.S.A.* 50, 697 (1944).
39. H.J. Monkhorst and J.D. Pack, *Phys. Rev. B* 13, 5188 (1976).
40. M. Methfessel and A.T. Paxton, *Phys. Rev. B* 40, 3616 (1989).
41. S.Q. Wang and H.Q. Ye, *Phys. Status Solidi (b)* 240, 45 (2003).
42. N. Arıkan, A. İyigör, A. Candan, Ş. Uğur, Z. Charifi, H. Baaziz, and G. Uğur, *J. Mater. Sci.* 49, 4180 (2014).
43. S. Baroni, P. Giannozzi, and A. Testa, *Phys. Rev. Lett.* 58, 1861 (1987).
44. F. Semari, F. Dahmane, N. Baki, Y. Al-Douri, S. Akbudak, G. Uğur, Ş. Uğur, A. Bouhemadou, R. Khenata, and C.H. Voon, *Chin. J. Phys.* 56, 567 (2018).

45. F. Taşkın, M. Atiş, O. Canko, S. Kervan, and N. Kervan, *J. Magn. Magn. Mater.* 426, 473 (2017).
46. A. Candan, S. Akbudak, Ş. Uğur, and G. Uğur, *J. Alloys Compd.* 771, 664 (2019).
47. Y. Feng and X. Xu, *J. Supercond. Nov. Magn.* 31, 1827 (2017).
48. O. Amrich, M.E.A. Monir, H. Baltach, S.B. Omran, X.W. Sun, X. Wang, Y. Al-Douri, A. Bouhemadou, and R. Khenata, *J. Supercond. Nov. Magn.* 31, 241 (2018).
49. A.A.M. Abadi, G. Forozani, S.M. Baizaee, and A. Gharaati, *J. Supercond. Nov. Magn.* 1-10 (2019).
50. T. Kanomata, M. Kikuchi, and H. Yamauchi, *J. Alloys Compd.* 414, 1 (2006).
51. P.D. Patel, S. Shinde, S.D. Gupta, S.D. Dabhi, and P.K. Jha, *Comput. Mater. Sci.* 15, 61 (2018).
52. P.D. Patel, S.M. Shinde, S.D. Gupta, and P.K. Jha, *Mater. Res. Express* 6, 076307 (2019).
53. W. Voigt, *Lehrbuch der Kristallphysik*, 2nd ed. (Berlin: LeipzigTeubner Verlag, 1928), p. 954.
54. A. Reuss, *ZAMM-Journal of Applied Mathematics and Mechanics/Zeitschrift für Angewandte Mathematik und Mechanik* 9, 49 (1929).
55. R. Hill, *Proc. Phys. Soc. Sec. A* 65, 349 (1952).
56. S.F. Pugh, *Dublin Philos. Mag. J. Sci.* 45, 823 (1954).
57. X.H. Kang and J.M. Zhang, *J. Phys. Chem. Solid.* 119, 71 (2018).
58. H. Fu, D. Li, F. Peng, T. Gao, and X. Cheng, *Comput. Mater. Sci.* 44, 774 (2008).
59. G. Surucu, *Mater. Chem. Phys.* 203, 106 (2018).
60. G. Surucu, K. Colakoglu, E. Deligoz, and N. Korozlu, *J. Elect. Mat.* 45, 4256 (2016).
61. G. Surucu, C. Kaderoglu, E. Deligoz, and H. Ozisik, *Mater. Chem. Phys.* 189, 90 (2017).
62. B. Kocak, Y.O. Ciftci, and G. Surucu, *J. Elect. Mat.* 46, 247 (2017).
63. X.Q. Chen, H. Niu, D. Li, and Y. Li, *Intermetallics* 19, 1275 (2011).
64. S.I. Ranganathan and M. Ostoja-Starzewski, *Phys. Rev. Lett.* 101, 055504 (2008).
65. P.D. Patel, S.B. Pillai, S.M. Shinde, S.D. Gupta, and P.K. Jha, *Phys. B Condens. Matter* 550, 376 (2018).
66. J. Wu, B. Zhang, and Y. Zhan, *J. Phys. Chem. Solid.* 104, 207 (2017).
67. A. Marmier, Z.A. Lethbridge, R.I. Walton, C.W. Smith, S.C. Parker, and K.E. Evans, *Comput. Phys. Commun.* 181, 2102 (2010).
68. K. Biswas and C.W. Myles, *Phys. Rev. B* 75, 245205 (2007).
69. H.B. Ozisik, K. Colakoglu, G. Surucu, and H. Ozisik, *Comp. Mater. Sci.* 50, 1070 (2011).
70. P. Wachter, M. Filzmoser, and J. Rebizant, *Phys. B Condens. Matter* 293, 199 (2001).
71. O.L. Anderson, *J. Phys. Chem. Solid.* 24, 909 (1963).
72. O.L. Anderson, E. Schreiber, and N. Soga, *Elastic Constants and Their Measurements* (1973).
73. M.E. Fine, L.D. Brown, and H.L. Marcus, *Scr. Metal.* 18, 951 (1984).

Publisher's Note Springer Nature remains neutral with regard to jurisdictional claims in published maps and institutional affiliations.